Requirement for *Lim1* in head-organizer function

William Shawlot & Richard R. Behringer*

Department of Molecular Genetics, The University of Texas M. D. Anderson Cancer Center, Houston, Texas 77030, USA

***Lim1* is a homeobox gene expressed in the organizer region of mouse embryos. To investigate the role of *Lim1* during embryogenesis, a targeted deletion of the *Lim1* gene was generated in embryonic stem cells. Embryos homozygous for the null allele lacked anterior head structures but the remaining body axis developed normally. A partial secondary axis developed anteriorly in some mutant embryos. *Lim1* is thus an essential regulator of the vertebrate head organizer.**

THE vertebrate organizer was originally described almost 70 years ago[1], when it was found that the dorsal blastopore lip of an amphibian gastrula-stage embryo could change the fate of surrounding cells and cause the formation of a secondary body axis when transplanted into an indifferent region of a host embryo; because of these remarkable inductive properties, the dorsal blastopore lip was dubbed the organizer[1].

Functionally equivalent organizing regions have been identified in chick and mouse embryos. These regions, Hensen's node in the chick and the node in the mouse, are located at the anterior end of the primitive streak and can cause the formation of a second neural axis when transplanted to the lateral region of a host embryo[2,3]. The molecular mechanisms involved in organizing the vertebrate body axis appear to be evolutionarily conserved, as Hensen's node can induce the expression of region-specific neural markers in *Xenopus* ectoderm[4] and transplantation of the distal tip of a streak-stage mouse embryo (which includes the presumptive node) to the blastocoel cavity of a *Xenopus* gastrula-stage embryo is reported to induce the formation of a secondary axis[5].

In an effort to understand the organizer at a molecular level, several genes encoding presumptive DNA transcription factors that are expressed in the *Xenopus*, chick and mouse organizer regions have been identified. These include *goosecoid*[5-7], the forkhead-motif-containing genes *XFH1/Pintallavis* in *Xenopus*[8,9] and the closely related *HNF3β* in mouse[10,11] and the *Xenopus* homeobox-containing gene *Xnot*[12,13]. The *Xenopus* homeobox gene *Xlim-1* is also expressed in the organizer region[14]. *Xlim-1* encodes a LIM class homeodomain motif and two cysteine-rich LIM domains which were first recognized as conserved motifs in the proteins encoded by *lin-11* in *Caenorhabditis elegans*[15], *Isl-1* in rat[16] and *mec-3* in *C. elegans*[17]. *Xlim-1* is initially expressed in the early dorsal blastopore lip and in the anterior-most dorsal mesoderm that underlies the future head region. Later *Xlim-1* is expressed in the developing kidney and portions of the central nervous system[18]. Injection of *Xlim-1* constructs that contain point mutations in the LIM domains into *Xenopus* embryos can induce neural differentiation in animal explants and can induce secondary axis formation when ectopically expressed in the ventral side of whole embryos[19].

The mouse homologue of *Xlim-1*, *Lim1*, has been cloned[20,21]. It shares 92% similarity with *Xlim-1* at the amino-acid level and is expressed in the node, the developing kidney and portions of the central nervous system. To determine whether *Lim1* has an essential role in organizer function, we generated *Lim1*-null mice by gene targeting in embryonic stem (ES) cells. We found that $Lim1^{-/-}$ embryos lacked anterior head structures but that the remaining body axis developed normally. The mutant embryos lacked forebrain and midbrain because of the absence of an organized node, head process and prechordal mesoderm in embryonic day (E) 7.5 embryos. Disruption of the early organizing region also caused a partial anterior secondary axis to develop in some mutant embryos. These results show that *Lim1* is an essential regulator of the vertebrate head organizer.

Early *Lim1* expression

To define more precisely the expression pattern of *Lim1* during early gastrulation, E6.5–7.0 embryos (pre-streak to late-streak stages) were examined by whole-mount RNA *in situ* hybridization. At the very early streak stage, *Lim1* was expressed in a small focused region of the epiblast where the primitive streak forms (Fig. 1*a*). At the early and mid-streak stages, *Lim1* was expressed in the mesodermal wings and in the primitive streak (Fig. 1*b*, *c*). By the mid-streak stage, *Lim1* expression could also be detected in the anterior mesoderm. At the late-streak stage, *Lim1* was expressed in the primitive streak and in the prechordal mesoderm (Fig. 1*d*). Expression of *Lim1* at the site in the epiblast where the primitive streak forms and in the migrating mesodermal wing, which comes to lie in the future head region, appears to be analogous to the expression of *Xlim-1* in the dorsal lip and the anteriorly migrating dorsal mesoderm during *Xenopus* gastrulation.

Lim1 phenotype

A *Lim1* null allele was generated by gene targeting in ES cells using a replacement vector that contained 5.5 kilobases (kb) of homology to the *Lim1* locus (Fig. 2*a*). Correct targeting results in the replacement of the entire *Lim1* coding region with PGKneo, thereby creating a null allele. Forty-one of 384 G418/FIAU-resistant clones were correctly targeted, as verified by Southern blot analysis (Fig. 2*b*). Eight independent targeted clones were injected into C57BL/6 blastocysts and two clones, 3B1 and 4G3, gave rise to chimaeric mice capable of transmission of the targeted allele through the germ line.

$Lim1^{-/-}$ embryos from both lines 3B1 and 4G3 had identical phenotypes. The analysis reported here is primarily of the 3B1 mice. Mice heterozygous for the targeted mutation appeared normal and were intercrossed to produce homozygous (−/−) embryos (Fig. 2*c*, top panel). Southern blot analysis using a *Lim1* complementary DNA fragment confirmed that the expected *Lim1* coding sequences were deleted (Fig. 2*c*, lower panel). Embryos from heterozygous intercrosses were initially examined at E9.5. $Lim1^{-/-}$ embryos lacked head structures just anterior to the otic vesicle (Fig. 3*a*). The rest of the body axis, however, appeared normal. Somites were present in the trunk and tail, and a beating heart was observed in most $Lim1^{-/-}$ embryos. Subsequent crosses of F_2 females with F_1 males yielded E9.5 $Lim1^{-/-}$ embryos that were smaller than wild-type embryos, had not completed embryonic turning and sometimes had kinks in their spinal cords (Fig. 4*f*). In some of these

* To whom correspondence should be addressed.

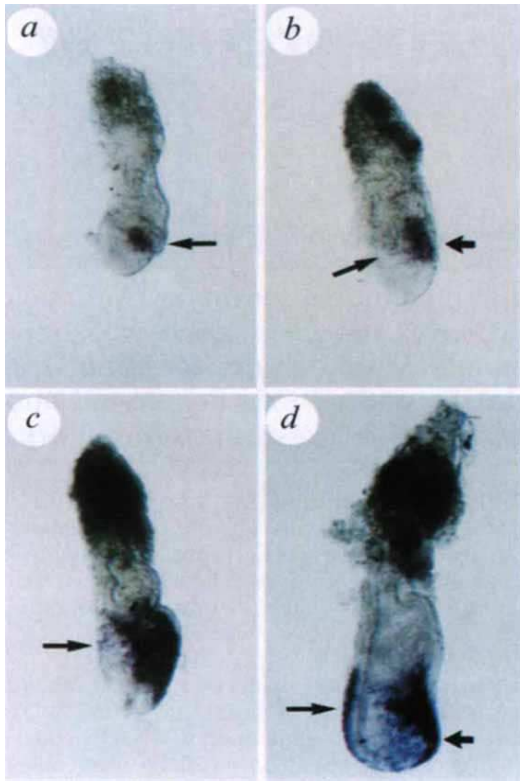

FIG. 1 Expression of *Lim1* from early to late primitive-streak stages revealed by whole-mount RNA *in situ* hybridization. *a*, Very-early-streak-stage embryo showing focused expression in the epiblast where primitive streak formation occurs (arrow). *b*, Early-streak stage. *Lim1* expression is present in the mesodermal wings (arrow) and in the primitive streak (short arrow). *c*, Mid-streak stage. Expression is present in the primitive streak, mesodermal wings and in the anterior mesoderm (arrow). *d*, Late-streak stage. *Lim1* expression is present in the primitive streak (short arrow) and in the prechordal mesoderm (arrow) which underlies the anterior portion of the future head.
METHODS. Whole-mount RNA *in situ* hybridization was done as described[43] using a 2.4-kb *Lim1* cDNA fragment containing the entire *Lim1* coding region. Embryos from outbred mice (Swiss) were collected at several time points between E6.5 and E7.0 and staged according to ref. 44.

embryos the allantois was shorter than normal and abnormally distended (data not shown). As the analysis was of 129 × C57BL/6 hybrid mice, the differences between F_2 and F_3 embryos could have been due to genetic background. But the loss of head structures just anterior to the otic vesicle was completely penetrant in all crosses.

When embryos from heterozygous intercrosses were examined at E10.5, *Lim1*$^{-/-}$ embryos in the process of being resorbed were found. This suggested that *Lim1*$^{-/-}$ embryos died at ~E10. Surprisingly, however, four headless *Lim1*$^{-/-}$ pups were delivered stillborn from the ~1,000 pups generated by intercrossing *Lim1* heterozygotes. With the exception of the head, the *Lim1*$^{-/-}$ stillborn pups appeared to be normal (Fig. 3*b*). Necropsies revealed that they lacked kidneys and gonads (data not shown) but all other gut structures, organs and tissues were present and appeared to be normal.

To confirm that *Lim1*$^{-/-}$ embryos were not surviving until birth only to be immediately cannibalized by their mothers, we killed pregnant females between days 10.5 and 14.0 of pregnancy and found no viable headless embryos in 14 litters, indicating that most *Lim1*$^{-/-}$ embryos died around E10.

Anterior neural-tissue formation

To determine whether or not anterior neural tissues are present in *Lim1*$^{-/-}$ embryos, we examined the expression of three neural markers: *Otx2*, *En* (*En1* and *En2*) and *Krox20*. At E8.5, *Otx2* is expressed in the forebrain and midbrain region in wild-type embryos[22] (Fig. 4*a*). E8.5 *Lim1*$^{-/-}$ embryos did not express *Otx2* (Fig. 4*b*). At earlier stages, there was no expression of *Otx2* in E7.5 headfold-stage *Lim1*$^{-/-}$ embryos but expression could be detected in the anterior portion of streak-stage *Lim1*$^{-/-}$ embryos (data not shown). As *Otx2* is initially expressed in the entire

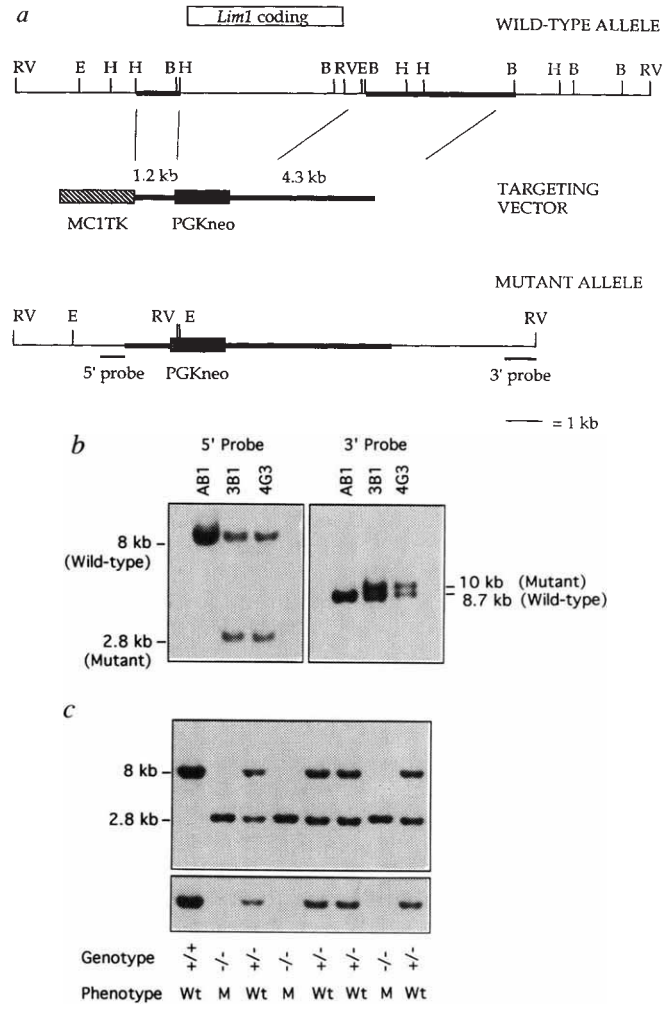

FIG. 2 Targeted deletion of the *Lim1* gene. *a*, Schematic representation of targeting. The 5.4-kb *Lim1*-coding region (W.S. and R.B. unpublished) was replaced with the PGKneobpa cassette[45] and flanked by 1.2 kb of 5′ *Lim1* homology and 4.3 kb of 3′ *Lim1* homology (thick black lines). The MC1TKpA herpes simplex virus thymidine kinase expression cassette[46] was inserted outside the short arm of homology for negative selection[47]. Correct targeting should result in the deletion of the entire *Lim1* protein-coding sequences. The *neo* cassette introduces novel *Eco*RI and *Eco*RV sites that allow genotyping by Southern analysis. B; *Bam*HI, E; *Eco*RI H; *Hin*dIII RV; *Eco*RV. *b*, Southern blot analysis of two targeted ES cell clones 3B1 and 4G3. DNA from G418- and FIAU (1-(2′-deoxy-2′-fluoro-β-D-arabinofuranosyl)-5-iodouracil)-resistant clones was digested with *Eco*RI for hybridization with the 5′ probe and with *Eco*RV for hybridization with the 3′ probe. AB1 ES cell DNA was included as a control. *c*, Southern blot analysis of DNA isolated from the yolk sacs of E9.5 embryos derived from a *Lim1* heterozygous intercross. Yolk sac DNA was digested with *Eco*RI and analysed by Southern blotting using the 5′ probe (top). The Southern blot was stripped and rehybridized with a 1.2-kb *Kpn*I–*Eco*RI *Lim1* cDNA fragment containing the entire protein-coding region of the gene apart from the first LIM domain (lower panel).
METHODS. Genomic DNA from a 129 genomic library was used to construct the targeting vector. The linearized vector was electroporated into 1×10^7 AB1 ES cells that were then selected for resistance to G418 and FIAU[46]. G418- and FIAU-resistant clones were screened for correct targeting by Southern analysis[48]. Targeted ES cell clones were injected into C57BL/6 blastocysts to generate chimaeric mice[49].

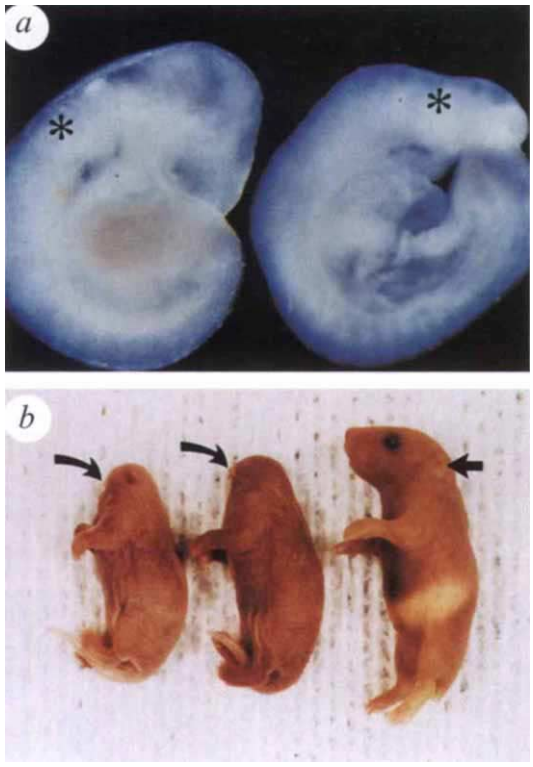

FIG. 3 Headless phenotype in *Lim1*$^{-/-}$ mice. *a*, *Lim1*$^{-/-}$ phenotype at E9.5. The wild-type embryo (*Lim1*$^{+/+}$ or *Lim1*$^{+/-}$) is shown on the left and the mutant (*Lim1*$^{-/-}$) embryo on the right. The mutant embryo lacks head structures just anterior to the otic vesicle (asterisk), but the trunk and tail regions are well formed. Somites are present in the trunk and tail of the mutant embryo. *b*, *Lim1*$^{-/-}$ phenotype at birth. Two *Lim1*$^{-/-}$ pups born on the same day from different litters are shown on the left, and a wild-type pup (+/+) on the right. Only four headless stillborn pups have been found from >1,000 pups generated by intercrossing *Lim1* heterozygotes. The *Lim1*$^{-/-}$ pups are about the same size as the (+/+) pup and, with the exception of the head region, appear to be normal. The ear pinnae (arrows) are located at the extreme anterior end of the *Lim1*$^{-/-}$ pups and lie ventrally. The wild-type pup used here for comparison had its tail cut for DNA extraction in a separate experiment.

epiblast[23], *Otx2* expression in streak stage *Lim1*$^{-/-}$ embryos may represent residual expression. The second marker, *En*, is first expressed at E8.0 and marks the presumptive boundary between the midbrain and hindbrain[24] (Fig. 4*c*). Like *Otx2*, no *En* expression was observed in mutant (−/−) embryos (Fig. 4*d*). *Krox20* is expressed in rhombomeres 3 and 5 of the hindbrain between E8.5 and E9.5 (ref. 25) (Fig. 4*e*). In *Lim1*$^{-/-}$ embryos, *Krox20* expression corresponding to rhombomeres 3 and 5 was evident. The region expressing rhombomere 3 was located at the extreme anterior end of the embryo and was reduced in size (Fig. 4*f*). These neural marker studies indicate that *Lim1*$^{-/-}$ embryos lack forebrain and midbrain but have a portion of the hindbrain, and that the neural truncation occurs just anterior to rhombomere 3.

Node and axial mesoderm formation

As *Lim1* expression is associated with the initiation of gastrulation, we examined *Lim1*$^{-/-}$ embryos for the presence of a node, head process and prechordal mesoderm. A morphologically distinct node was present in E7.5 *Lim1*$^{+/+}$ and *Lim1*$^{+/-}$ neural-plate and headfold-state embryos (Fig. 5*a*, *c*). In contrast, no morphologically distinct node was present in any of the E7.5 *Lim1*$^{-/-}$ embryos (Fig. 5*b*, *d*). These embryos were usually immediately recognizable because the embryonic portion of the egg cylinder was smaller and a constriction existed between the embryonic and extraembryonic regions.

To find out whether *Lim1*$^{-/-}$ embryos express node- and axial mesoderm-related genes, we examined the expression of *Brachyury* and *HNF3β*. At E7.5, *Brachyury* is expressed in the node, the head process and the primitive streak[26] (Fig. 5*a*). In *Lim1*$^{-/-}$ embryos, *Brachyury* was expressed in the primitive streak but did not extend to the distal tip of the embryo. Node- and head-process-related expression were absent (Fig. 5*b*). At E7.5, *HNF3β* is expressed in the node, head process and prechordal mesoderm[10,11,27] (Fig. 5*c*). In *Lim1*$^{-/-}$ embryos, *HNF3β* expression was detected weakly in three of eight embryos near the posterior third of the embryo (Fig. 5*d*). Anterior expression corresponding to the head process and prechordal mesoderm was not detected.

We also analysed the expression of the node-specific marker *nodal*[28,29]. In E7.5 wild-type embryos, *nodal* is expressed in cells that lie at the periphery of the node (Fig. 5*e*). In E7.5 *Lim1*$^{-/-}$ embryos, weak expression was observed in four of five embryos near the posterior third of the embryo (Fig. 5*f*). The staining was diffuse and not restricted to cells at the periphery of the node as in wild-type embryos. In addition, we also examined the expression of *goosecoid*, which is evident in cells that have

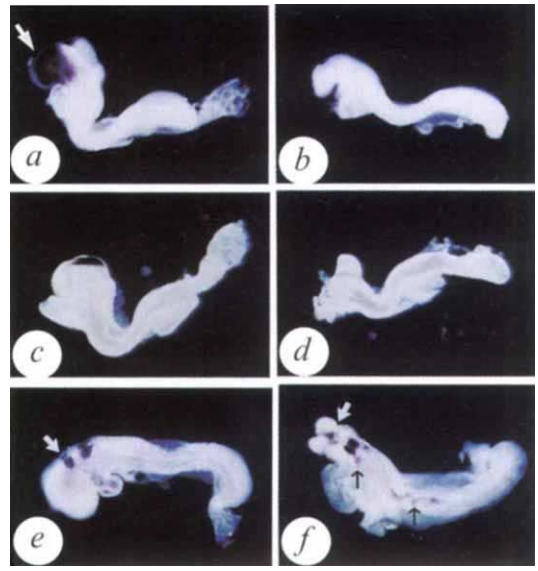

FIG. 4 Whole-mount analysis of anterior neural markers in *Lim1*$^{-/-}$ embryos between E8.0 and E9.5. *a*, *c* and *e*, *Lim1*$^{+/+}$ or *Lim1*$^{+/-}$ embryos; *b*, *d* and *f*, *Lim1*$^{-/-}$ embryos. Embryos are all oriented so that anterior is to the left and dorsal is up. *a* and *b*, *Otx2* expression in E8.5 embryos. *Otx2* is expressed in the forebrain and midbrain (arrow) of wild-type embryos (*a*) but is not present in *Lim1*$^{-/-}$ embryos (*b*). *c* and *d*, *En* (*En1* and *En2*) expression in E8.0 embryos. In wild-type embryos *En* is expressed at the presumptive midbrain/hindbrain boundary (*c*) but is absent in *Lim1*$^{-/-}$ embryos (*d*). *e* and *f*, *Krox20* expression in E9.5 embryos. *Krox20* is expressed in a region corresponding to rhombomeres 3 (white arrow) and 5 in both wild-type (e) and *Lim1*$^{-/-}$ embryos (*f*). The size of the *Krox20* expression domain in rhombomere 3 of the *Lim1*$^{-/-}$ embryo appears smaller. *Krox20* expression is also present in neural crest cells migrating from rhombomere 5 and the spinal ganglia[25] (black arrows).

METHODS. For whole-mount *in situ* hybridization, digoxigenin-labelled RNA probes for *Otx2* (ref. 22) and *Krox20* (ref. 24) were used. *En* marker was analysed by whole-mount immunohistochemistry using an antibody recognizing both En1 and En2 (ref. 50). Embryos at E8.5 and E9.5 were genotyped by Southern analysis of DNA isolated from the yolk sac. E8.0 embryos were genotyped by the polymerase chain reaction (PCR) using yolk sac DNA. The primers used for genotyping were 5′-CGTCCCAACTCACTACTAGAAACCG-3′ (1.2 kb, short arm), 5′-CTGTCAGAAGTCAAAGTGCATCTGC-3′ (deleted region) and 5′-AATCCATCTTGTTCAATGGCCGATC-3′ (ref. 45; neo). The size of the amplified products from the wild-type allele and mutant allele are 177 bp and 608 bp, respectively.

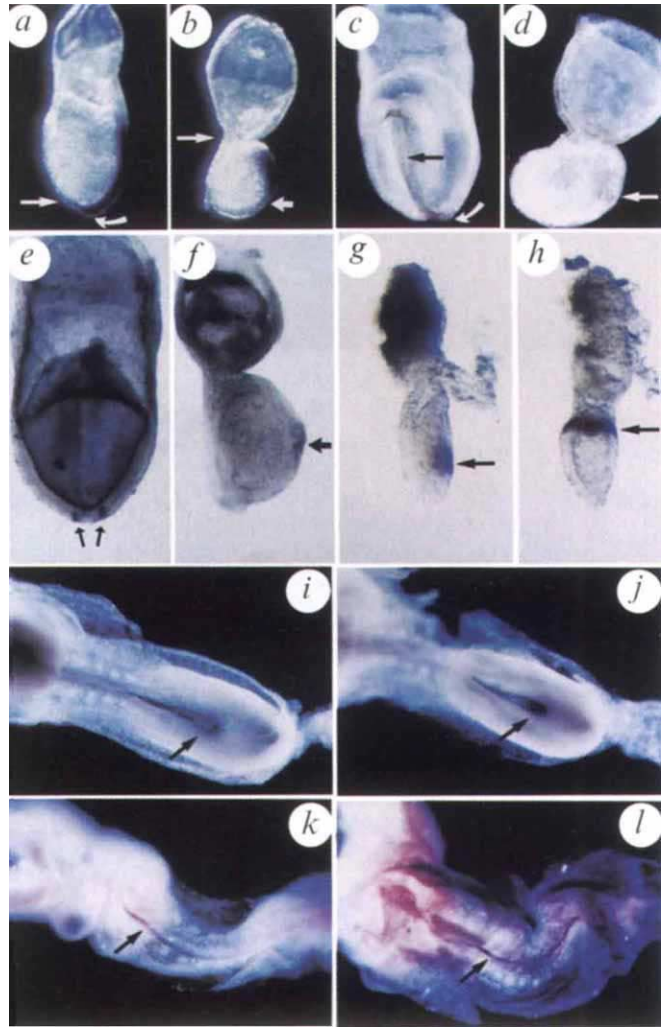

FIG. 5 Whole-mount analysis of node and axial mesoderm markers in *Lim1*$^{-/-}$ embryos. *a*, *c*, *e*, *g*, *i* and *k*, *Lim1*$^{+/+}$ or *Lim1*$^{+/-}$ embryos; *b*, *d*, *f*, *h*, *j* and *l*, *Lim1*$^{-/-}$ embryos (anterior is to the left and posterior to the right). *a* and *b*, Expression of *Brachyury* in E7.5 embryos at the neural-plate stage. *Brachyury* is expressed in the primitive streak, the node (curved arrow) and head process (straight arrow) in wild-type embryos (*a*). In mutant embryos, *Brachyury* expression is only in the primitive streak region. Short arrow marks the anterior extent of the streak, and the longer arrow the abnormal constriction between the embryonic and extraembryonic regions (*b*). *c* and *d*, Expression of *HNF3β* in E7.5 embryos at the headfold stage. In E7.5 wild-type embryos, *HNF3β* is expressed in the node (curved arrow) and head process (straight arrow) (*c*). In *Lim1*$^{-/-}$ embryos, there was either no expression or weak expression (3 of 8 mutant embryos) in a small patch in the posterior third of the embryo (arrow) (*d*). *e* and *f*, Expression of *nodal* in E7.5 embryos. The wild-type embryo (early headfold stage) is oriented so the neural plate is facing the viewer (*e*). The *Lim1*$^{-/-}$ embryos is oriented so anterior is to the left (*f*). The *nodal* staining region in both embryos is marked with arrows in *e* and a short arrow in *f*. *g* and *h*, *goosecoid* expression in E6.5 embryos. In the wild-type embryo (mid-streak stage) (*g*), *goosecoid* is expressed in the anterior portion of the primitive streak (arrow). In *Lim1*$^{-/-}$ embryos, *goosecoid*-expressing cells (arrow) are present between the embryonic and extra-embryonic portions of the embryo (arrow) (*h*). *i* and *j*, Expression of *HNF3β* in the node region of E8.5 embryos. *HNF3β* expression was observed in the node (arrow) of wild-type (*i*) and *Lim1*$^{-/-}$ embryos (*j*) (dorsal views). *k* and *l*, *Brachyury* expression in E8.5 embryos. *Brachyury* is expressed in the notochord in the trunk (arrow) and tail in both wild-type (*k*) and *Lim1*$^{-/-}$ embryos (*l*) (ventral views).
METHODS. *Brachyury*, *nodal* and *goosecoid* expression were detected by whole-mount RNA *in situ* hybridization; *HNF3β* expression was detected by whole-mount immunohistochemistry. The 630-bp *nodal* probe[28] and the *HNF3β* antibody were obtained from B. Hogan; pme68S (*Brachyury*) was from B. Herrmann. The *goosecoid* probe used was a 905-bp *Hin*cII/*Pst*I genomic fragment containing a portion of exon 2 and exon 3 (ref. 5).

organizer activity before the formation of a definitive node[5]. In E6.5 wild-type embryos (mid-streak stage), *goosecoid* is expressed in the anterior portion of the primitive streak[5] (Fig. 5*g*). In E6.5 *Lim1*$^{-/-}$ embryos, *goosecoid* was expressed, but *goosecoid*-expressing cells were localized to the region between the embryonic and extraembryonic portions of the embryo (Fig. 5*h*). The *goosecoid*-expressing region also appeared to be enlarged relative to the region of expression in wild-type embryos.

As the trunk and tail regions of *Lim1*$^{-/-}$ embryos formed essentially normally, we considered that an organized node might develop after E7.5. We therefore examined E8.5 embryos that had not yet completed embryonic turning for node-specific expression of *HNF3β*. At this stage in development, the node is located in the tail[30]. *HNF3β* expression in the node of *Lim1*$^{-/-}$ embryos was indistinguishable from expression in wild-type embryos (Fig. 5*i*, *j*). At E8.5, *Brachyury* serves as a marker for the notochord[31] (Fig. 5*k*). In *Lim1*$^{-/-}$ embryos, *Brachyury*

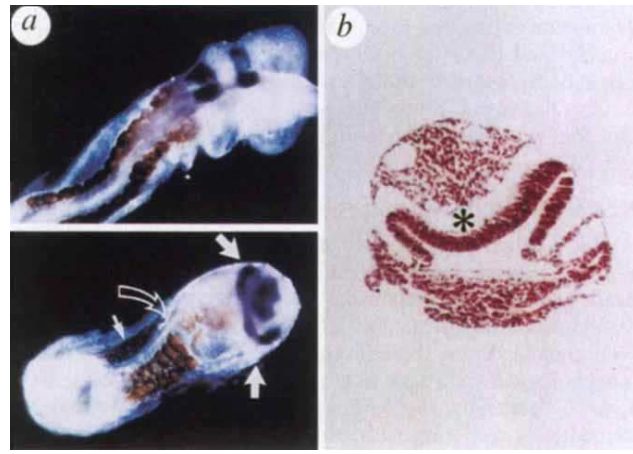

FIG. 6 Development of an anterior secondary axis in a *Lim1*$^{-/-}$ embryo. *a*, An E8.5 wild-type embryo (top) and *Lim1*$^{-/-}$ embryo (bottom) tested for *Krox20* and *Mox1* expression. In the wild-type embryo *Krox20* (purple) is expressed in rhombomere 3 and 5 and *Mox1* (brown) is expressed in the somites. In the *Lim1*$^{-/-}$ embryo, two neural axes could be discerned and are marked with large solid white arrows. The neural axes join in the mid-trunk region (curved arrow) and approach one another at the anterior end of the embryo. Two rhombomere-5 domains of *Krox20* expression are present on each side of the embryo and an enlarged rhombomere-3-staining region is also evident. Two columns of partially fused somites are seen on the right side of the embryo and a third column of somites (small white arrow) is present on the extreme lateral left side of the embryo. *b*, A transverse section through the anterior region of the mutant embryo in *a*, stained with haematoxylin and eosin. The neuroepithelium (asterisk) extends the width of the embryo and folds back on itself at the side of the embryo.
METHODS. Double-labelling was done by *in situ* hybridization for *Krox20* (ref. 25) followed by whole-mount immunohistochemistry using a Mox1 antibody (provided by C. Wright).

expression was detected along the midline of the trunk and tail (Fig. 5*l*).

Secondary axis formation

Of the ~60 *Lim1*$^{-/-}$ embryos examined between E8.5 and E9.5, three had a partial secondary axis. Secondary axis formation has not been observed in any *Lim1*$^{+/+}$ and *Lim1*$^{+/-}$ embryos. Although the axial duplications were slightly different between the three embryos, all three embryos lacked anterior head structures but had anterior neural duplications whose axes joined in the mid-trunk region. To visualize the secondary axis more clearly, one of the embryos was subjected to whole-mount *in situ* hybridization with a *Krox20* RNA probe, followed by whole-mount immunohistochemical analysis with an antibody against the somite-specific marker Mox1 (ref. 32) (Fig. 6*a*). In this *Lim1*$^{-/-}$ embryo, two independent *Krox20* rhombomere-5 domains of expression were located on each side of the embryo which formed an almost continuous band across the back of the embryo. Anteriorly, the neural axes converged at the end of the embryo and an enlarged *Krox20*-expressing region corresponding to rhombomere 3 was present. The Mox1 staining pattern showed that three columns of somites were present: one column of somites on the extreme lateral left side of the embryo and two columns that were partially fused on the right side of the embryo. In the anterior portion of the embryo, the columns of fused somites were located between the two neural axes. Histological sections from the anterior region of the embryo revealed a single neuroepithelium that spanned the width of the embryo and folded back on itself at the sides to form the neural axes initially observed (Fig. 6*b*). The notochord could not be conclusively identified in the sections.

Discussion

Our results demonstrate that *Lim1* is essential for head formation during mouse embryogenesis. *Lim1*$^{-/-}$ embryos lacked anterior head structures but the trunk and tail regions developed normally. This was most graphically demonstrated by the birth of several headless pups that were otherwise morphologically normal. Following the organizer experiment[1], Spemann[33] classified the organizer into a head organizer responsible for head formation and a trunk organizer responsible for body axis formation. The head organizer was composed of cells in the dorsal blastopore lip that initiate gastrulation and form head mesoderm; the trunk organizer was composed of cells that involute from the dorsal blastopore lip at the late gastrula stage and form notochord. This hypothesis was supported experimentally by the observation that organizer transplants of early gastrula dorsal lip regions, containing prospective head mesoderm, tended to give rise to secondary axes with head and brain structures, and transplants of late gastrula dorsal lip regions, containing prospective posterior mesoderm, tended to give rise to trunk and tail structures[34]. Our results indicate that *Lim1*$^{-/-}$embryos lacked an organized early node, head process and prechordal mesoderm but did develop an organized node structure by E8.5 and had a notochord. Because *Lim1*$^{-/-}$ embryos lacked head structures but their body axes developed normally, we propose that *Lim1* is a regulator of the head organizer.

Abnormalities in *Lim1*$^{-/-}$ embryos are apparent shortly after the onset of gastrulation, as demonstrated by the abnormal location of *goosecoid*-expressing cells in E6.5 *Lim1*$^{-/-}$ embryos. The presence of *goosecoid*-expressing cells between the embryonic and extraembryonic portions of the embryo suggests that an organizing region was formed but that early gastrulation movements were affected. This observation is of particular interest because the truncation of anterior head structures in *Lim1*$^{-/-}$ embryos is similar to the phenotypic effects observed in *Xenopus* embryos when gastrulation movements are blocked by the injection of polysulphonated compounds such as trypan blue or suramine[35]. Abnormal gastrulation movements of cells with altered organizing abilities may also explain why a secondary axis was observed in ~5% of E8.5 *Lim1*$^{-/-}$ embryos. The self-regulative capacities of the embryo may account in part for the low frequency of secondary axis formation.

An organized node structure does not form in E7.5 *Lim1*$^{-/-}$ embryos. This may be because the initial organizer region is not specified correctly or because gastrulation movements are abnormal. At E7.5 the primitive streak had extended about half way down the posterior side of *Lim1*$^{-/-}$ embryos, as demonstrated by the presence of *Brachyury* expression. Expression of *Brachyury* in a node structure at the end of the streak was not seen, although weak *HNF3β* and *nodal* could sometimes be detected in this region. *nodal* expression in *Lim1*$^{-/-}$ embryos was present as a diffuse region instead of being present on the periphery of the node as in wild-type embryos. These results imply that a node was present but that it was not organized correctly. As the head process is believed to be derived from the anterior portion of the primitive streak at the late-streak stage[36], the absence of the head process in *Lim1*$^{-/-}$ embryos is not unexpected. The fate of the head process is not clear, although it may give rise to the notochord[37], prechordal mesoderm[38] and part of the gut endoderm[39]. We did not examine endoderm or gut markers in *Lim1*$^{-/-}$ embryos, but the normal gut structure in the headless newborn pups suggests that the formation of definitive endoderm was unimpaired.

Classical experiments[40] suggest that the mesoderm anterior to the notochord is responsible for the induction of the forebrain, whereas the notochord is responsible for the induction of the hindbrain, spinal cord and possibly the midbrain. As *HNF3β* is also expressed in the prechordal mesoderm region at E7.5 (refs 10, 11, 27), the absence of *HNF3β* expression at the anterior end of *Lim1*$^{-/-}$ embryos suggests that the prechordal mesoderm is absent. Although planar signals from the organizer region may also be involved in neural induction and patterning in *Xenopus*, the lack of eye development in exogastrulae and Keller explant experiments suggests that vertical signals from the prechordal mesoderm could be necessary for forebrain development[41]. Our results provide genetic evidence that the prechordal mesoderm is required for forebrain development, but also that it may be required for midbrain development as well.

Two groups have reported the effects of targeted mutations in *HNF3β* (refs 27, 42). *HNF3β*$^{-/-}$ embryos lack a notochord, have abnormal dorsal–ventral patterning of the neural tube and defective foregut morphogenesis. The primary defect in *HNF3β*$^{-/-}$ embryos, like *Lim1*$^{-/-}$ embryos, is the absence of a organized node and head process, causing the head region to develop abnormally. One significant difference between *Lim1* and *HNF3β* mutants is that, despite the absence of a defined head process, some *HNF3β*$^{-/-}$ embryos express the anterior neural marker genes *Otx2* and *En*, but the reason for this difference is not known. Although the head process may give rise to prechordal mesoderm[38], the early expression pattern of *Lim1* in the mesodermal wings and then in the prechordal mesoderm suggests that cells in the mesodermal wings contribute at least in part to the formation of the prechordal mesoderm. One explanation for the expression of anterior neural markers in *HNF3β*$^{-/-}$ embryos is that, despite the absence of a defined head process, some *Lim1*-expressing cells from the mesodermal wings may be present in the anterior of the embryo. However, no obvious anterior expression of *Lim1* has been detected in *HNF3β*$^{-/-}$ embryos (S.-L. Ang, personal communication).

In the *Lim1*$^{-/-}$ mice that were born, necropsy revealed the absence of kidneys and gonads. As *Lim1* is expressed in the developing kidney[20,21], the absence of these structures is unlikely to be secondary to the node defects. Because most *Lim1*$^{-/-}$ embryos died around E10, we have not yet been able to analyse the urogenital phenotype thoroughly. *Lim1*$^{-/-}$ embryos probably died at E10 because the allantois was short and distended and did not fuse with the chorion.

In summary, *Lim1*-deficient mice show that *Lim1* is required for formation of an early organized node and anterior axial

mesoderm during mouse embryogenesis. Their headless phenotype indicates that *Lim1* is an essential regulator of the head organizer. These mice will be an important genetic tool for the molecular and cellular analysis of axis formation and neural induction during vertebrate embryogenesis. □

Received 21 December 1994; accepted 17 February 1995.

1. Spemann, H. & Mangold, H. *Wilhelm Roux Arch. Entw. Mech. Org.* **100,** 599–638 (1924).
2. Waddington, C. H. *J. exp. Biol.* **10,** 38–46 (1932).
3. Beddington, R. S. P. *Development* **120,** 613–620 (1994).
4. Kintner, C. R. & Dodd, J. *Development* **113,** 1495–1505 (1991).
5. Blum, M. *et al. Cell* **69,** 1097–1106 (1992).
6. Cho, K. W. Y., Blumberg, B., Steinbeisser, H. & De Robertis, E. M. *Cell* **67,** 1111–1120 (1991).
7. Izpisua-Belmonte, J. C., DeRobertis, E. M., Storey, K. G. & Stern, C. D. *Cell* **74,** 645–659 (1993).
8. Dirksen, M. L. & Jamrich, M. *Genes Dev.* **6,** 599–608 (1992).
9. Ruiz i Altaba, A. & Jessel, T. M. *Development* **116,** 81–93 (1992).
10. Sasaki, H. & Hogan, B. L. M. *Development* **118,** 47–59 (1993).
11. Ang, S.-L. *et al. Development* **119,** 1301–1315 (1993).
12. von Dassow, G., Schmidt, J. E. & Kimmelman, D. *Genes Dev.* **7,** 355–366 (1993).
13. Gont, L. K., Steinbeisser, H., Blumberg, B. & DeRobertis, E. M. *Development* **119,** 991–1004 (1993).
14. Taira, M., Jamrich, M., Good, P. J. & Dawid, I. B. *Genes Dev.* **6,** 356–366 (1992).
15. Freyd, G., Kim, S. K. & Horvitz, H. R. *Nature* **344,** 876–879 (1990).
16. Karlsson, O., Thor, S., Norberg, T., Ohlsson, H. & Edlund, T. *Nature* **344,** 879–882 (1990).
17. Way, J. C. & Chalfie, M. *Cell* **54,** 5–16 (1988).
18. Taira, M., Otani, H., Jamrich, M. & Dawid, I. B. *Development* **120,** 1525–1536 (1994).
19. Taira, M., Otani, H., Saint-Jeannet, J.-P. & Dawid, I. B. *Nature* **372,** 677–679 (1994).
20. Barnes, J. D., Crosby, J. L., Jones, C. M., Wright, C. V. E. & Hogan, B. L. M. *Devl Biol.* **161,** 168–178 (1994).
21. Fujii, T. *et al. Dev. Dynamics* **199,** 73–83 (1994).
22. Simeone, A., Acampora, D., Gulisano, M., Storaiuolo, A. & Bonicelli, E. *Nature* **358,** 687–690 (1992).
23. Ang, S.-L., Conlon, R. A., Jin, O. & Rossant, J. *Development* **120,** 2979–2989 (1994).
24. Davis, C. A. & Joyner, A. L. *Genes Dev.* **2,** 1736–1744 (1988).
25. Wilkinson, D., Bhatt, S., Chavrier, P., Bravo, R. & Charnay, P. *Nature* **337,** 461–464 (1989).
26. Herrmann, B. G. *Development* **113,** 913–917 (1991).
27. Weinstein, D. C. *et al. Cell* **78,** 575–588 (1994).
28. Zhou, X. *et al. Nature* **361,** 543–547 (1993).
29. Conlon, F. L. *et al. Development* **120,** 1919–1928 (1994).
30. Theiler, K. *The House Mouse: Atlas of Embryonic Development* (Springer, New York, 1989).
31. Wilkinson, D. G., Bhatt, S. & Herrmann, B. G. *Nature* **343,** 657–659 (1990).
32. Candia, A. H. *et al. Development* **116,** 1123–1136 (1992).
33. Spemann, H. *Naturwissenschaften* **15,** 946–951 (1927).
34. Spemann, H. *Wilhelm Roux Arch. Entw. Mech. Org.* **123,** 389–517 (1931).
35. Gerhart, J., Doniach, T. & Stewart, R. in *Gastrulation: Movements, Patterns and Molecules* (eds Keller, R., Clark, W. H. Jr & Griffin, F.) 57–77 (Plenum, New York, 1991).
36. Beddington, R. S. P. in *Postimplantation Development in the Mouse* (eds Chadwick, D. J. & Marsh, J.) 55–58 (Wiley, Chichester, 1992).
37. Jurand, A. *J. Embryol. exp. Morph.* **32,** 1–33 (1974).
38. Meir, S. & Tam, P. P. L. *Differentiation* **117,** 96–98 (1982).
39. Tam, P. P. L. & Beddington, R. S. P. in *Postimplantation Development in the Mouse* (eds Chadwick, D. J. & Marsh J.) 27–49 (Wiley, Chichester, 1992).
40. Yamada, T. *Development* **120,** 3051–3062 (1994).
41. Riuz i Altaba, A. *J. Neurobiol.* **24,** 1276–1304 (1993).
42. Ang, S.-L. & Rossant, J. *Cell* **78,** 561–574 (1994).
43. Wilkinson, D. G. in *In Situ Hybridization* (ed. Wilkinson, D. G.) 75–83 (IRL, Oxford, 1992).
44. Downs, K. M. & Davies, T. *Development* **118,** 1255–1266 (1993).
45. Soriano, P., Montgomery, C., Geske, R. & Bradley, A. *Cell* **64,** 694–702 (1991).
46. McMahon, A. P. & Bradley, A. *Cell* **62,** 1073–1085 (1990).
47. Mansour, S. L., Thomas, K. R. & Capecchi, M. R. *Nature* **336,** 348–352 (1988).
48. Ramirez-Solis, R. *et al. Analyt. Biochem.* **201,** 331–335 (1992).
49. Bradley, A. in *Teratocarcinomas and Embryonic Stem Cells* (ed. Robertson, E. J.) 113–151 (IRL, Oxford, 1987).
50. Davis, C. A., Holmyard, D. P., Millen, K. J. & Joyner, A. L. *Development* **111,** 287–298 (1991).

ACKNOWLEDGEMENTS. We thank B. Herrmann, B. Hogan, A. Joyner, J. Rossant and C. Wright for probes and antibodies; A. Bradley for AB1 ES cells and SNL76/7 STO fibroblast cells; J. Deng for assistance with tissue culture; and M. Goode and C. Wright for their comments on the manuscript. This work was supported by an NIH training grant to W.S. and grants from the Sid W. Richardson Foundation and the NIH to R.R.B.

LETTERS TO NATURE

Detecting intergalactic magnetic fields using time delays in pulses of γ-rays

R. Plaga

Max-Planck-Institut für Physik, Föhringer Ring 6, 80805 Munich, Germany

INTERGALACTIC magnetic fields (IGMFs) can be produced by a number of mechanisms, but are expected to be weak and have not so far been detected. 'Primordial' magnetic fields might have been produced in the very early Universe, either by quantum fluctuations during the 'inflationary' period[1,2] or through the decoupling transitions of the fundamental forces[3,4]. The much later ejection of magnetized plasma into intergalactic space from galaxies and active galactic nuclei should also produce IGMFs, though it is possible that some fraction of the Universe retains its 'primordial' field[5]. Previous studies[6] have placed an upper limit of 10^{-9} gauss on the strength of an IGMF (with a coherence length of 1 Mpc), but the strength may be much less than this, posing a formidable challenge to current observational capabilities. Here I propose a highly sensitive method for probing weak IGMFs by exploiting their effect on the arrival times of γ-rays from extragalactic sources. The delay in arrival owing to the action of intergalactic magnetic fields on electron cascades caused by scattering of the γ-ray photons might be used to measure fields as weak as 10^{-24} gauss. I suggest that this effect may already have been seen in the arrival times of high-energy photons after the main burst of a γ-ray burster[7].

The γ-rays emitted by extragalactic sources suffer photon–photon collisions in diffuse electromagnetic background radiation fields, leading to particle pair production[8]. At γ-ray energies from ~100 GeV to 100 TeV pair production involving infrared background radiation (the intensity of which is not well known) dominates. The mean free path length is comparable to the distance of the farthest objects in the Universe for photons of ~100 GeV and falls at higher energies (for example, to 10–300 Mpc at 100 TeV) depending on the intensity of the infrared background[9]. The particle pairs produced scatter elastically off photons of the 2.7 K microwave background radiation boosting their energy via the inverse Compton effect, so that a pair–photon cascade develops[10].

Electrons and positrons (called collectively 'electrons' below) drifting through IGMFs are deflected. An extragalactic source of γ-rays with short, well defined periods of greatly enhanced luminosity ('pulses' of γ-rays) will therefore be characterized by: (1) a prompt pulse of γ-rays which does not interact with background photons to form charged particles, and which therefore does not suffer any deflection; (2) a delayed 'after pulse' (called FID for 'field-induced delay') of cascade photons arising from the inverse Compton scattering of electrons deflected by the IGMF. 'Cascade' photons have to cross a larger distance to reach the observer than do photons arriving directly from the source, and so arrive correspondingly later.

If the FID is much larger than the duration of the prompt pulse, it will be possible to study the events in the FID exclusively. At energies above ~0.01 GeV, the photons of the pair–photon cascade can form a significant fraction of the total signal from cosmological sources with source spectra extending to very high energies[9]. It is in this energy range that one should look for the FIDs.

There are two classes of sources of 'γ-ray pulses' in this energy range, which cover a wide range of pulse durations. Objects related to active galactic nuclei (for example, the quasar 3C279 exhibited[11] flaring activity on a timescale of days to months in 1991–92), and γ-ray bursters (GRBs) which exhibit intensity variations on timescales from milliseconds to minutes[12]. In the former case, it is certain that some have spectra extending into the very-high-energy region (VHE) above ~10 GeV as the nearby active galactic nucleus Markarian 421 has been detected[13] at energies of up to 3 TeV. Currently the most favoured hypothesis is that GRBs are located at cosmological distances[14]. As